

Supplementary Information

**Mechanics Induced Triple-mode Anticounterfeiting and Moving  
Tactile Sensing by Simultaneously Utilizing Instantaneous and  
Persistent Mechanoluminescence**

Zhidong Ma,<sup>a,b</sup> Jinyu Zhou,<sup>a</sup> Jiachi Zhang,<sup>\*a</sup> Songshan Zeng,<sup>c</sup> Hui Zhou,<sup>b</sup> Andrew T. Smith,<sup>c</sup>

Wenxiang Wang,<sup>a</sup> Luyi Sun<sup>c</sup> and Zhaofeng Wang<sup>\*b</sup>

*<sup>a</sup> National & Local Joint Engineering Laboratory for Optical Conversion Materials and  
Technology, Lanzhou University, Lanzhou 730000, P. R. China*

*<sup>b</sup> State Key Laboratory of Solid Lubrication, Lanzhou Institute of Chemical Physics, Chinese  
Academy of Sciences, Lanzhou 730000, P. R. China*

*<sup>c</sup> Polymer Program, Institute of Materials Science and Department of Chemical &  
Biomolecular Engineering, University of Connecticut, Storrs, Connecticut 06269, USA*

\*Authors to whom correspondence should be addressed:

Dr. Jiachi Zhang, Tel.: +86-931-8912772; Email: zhangjch@lzu.edu.cn

Dr. Zhaofeng Wang, Tel: +86-931-4968682; Email: zhfwang@licp.cas.cn

## 1. Experimental details

### 1.1 ML powders

YAG: 2.5%Ce<sup>3+</sup> and BSSON: 6%Eu<sup>2+</sup> were employed as the ML materials in this work, which were synthesized by a solid-state reaction. For YAG: 2.5%Ce<sup>3+</sup>, the starting materials were Y<sub>2</sub>O<sub>3</sub> (99.99%), Al<sub>2</sub>O<sub>3</sub> (99.99%) and CeO<sub>2</sub> (99.99%). First, the stoichiometric raw materials were weighed and thoroughly ground in an agate mortar with the assistance of ethanol. Then, the mixture was transferred in a corundum crucible, and sintered at 1575 °C for 6 h in a horizontal tube furnace under a flowing atmosphere of forming gas (90% N<sub>2</sub>, 10% H<sub>2</sub>). After cooling to room temperature, YAG: 2.5%Ce<sup>3+</sup> ML powders were obtained.

For BSSON: 6%Eu<sup>2+</sup> samples, the starting materials were BaCO<sub>3</sub> (99.9%), SrCO<sub>3</sub> (99.9%), EuF<sub>3</sub> (99.5%) and α-Si<sub>3</sub>N<sub>4</sub> (99.5%). After thoroughly mixing the stoichiometric raw materials in an agate mortar, the mixture was put in a zirconia crucible, and sintered at 1650 °C for 4 h under a flowing atmosphere of forming gas (90% N<sub>2</sub>, 10% H<sub>2</sub>). After cooling to room temperature, BSSON: 6%Eu<sup>2+</sup> ML powders were obtained.

For the control samples, ZnS: Mn<sup>2+</sup> powders were synthesized according to our previous report.<sup>[40]</sup> The well-known ZnS: Cu<sup>2+</sup>, SrAl<sub>2</sub>O<sub>4</sub>: Eu<sup>2+</sup> and Sr<sub>2</sub>MgSi<sub>2</sub>O<sub>7</sub>: Eu<sup>2+</sup> were purchased from Foshan xiucui chemicals Co., Ltd.

### 1.2 Fabrication of ML elastomers.

PDMS (Sylgard 184, Dow Corning) was employed as the elastic matrix to provide interior stress for ML powders. First, 1.5 g of PDMS base resin and 0.15 g of curing agent were mixed in a petri dish with a diameter of 60 mm. Then, 3 g of ML powders were dispersed in above mixture by mechanical stirring for 5 min. After curing at 80 °C for 2 h, the PDMS-

based ML elastomers were obtained.

### **1.3 Fabrication of triple-mode anticounterfeiting device**

The as-obtained YAG: Ce<sup>3+</sup>/PDMS and BSSON: Eu<sup>2+</sup>/PDMS elastomers were cut into strips, representing various anticounterfeiting information. The strips were then placed in a petri dish (diameter: 60 mm) filled with pure PDMS precursors for another curing at 80 °C for 2 h. Finally, the cured elastomer with ML patterns was peeled off carefully and the triple-mode anticounterfeiting device was fabricated.

### **1.4 Fabrication of tactile sensor.**

In the case of plane sensor, 2 g of YAG: Ce<sup>3+</sup> and 1 g of BSSON: Eu<sup>2+</sup> powders were mixed together with 2 g of PDMS base resin and 0.2 g of curing agent in a petri dish with a diameter of 60 mm. After mechanical stirring for 5 min, the above mixture was cured at 80 °C for 2 h, and the plane tactile sensor was obtained.

To further improve the discernibility of the above sensor, ML elastic arrays were fabricated on the surface. First, a polylactic acid (PLA) model with arrays of holes (100 holes, hole diameter: 2 mm, hole depth: 5mm, hole spacing: 1 mm) was acquired by a commercial desktop 3D printer (Raise3D N2). Then, the ML mixture, as described in the above case of plane tracking device, was injected into the holes on the model. After curing at 80 °C for 2 h, the elastomer was peeled off and the comprehensive tactile sensor composed of ML arrays was obtained.

### **1.5 Characterizations.**

The XRD patterns of the ML powders were collected by an X-ray diffractometer (Rigaku D\Max-2400) with Ni-filtered Cu K $\alpha$  radiation. The morphology and microstructure of the ML

composites were examined by SEM (S-340, Hitachi, Japan). The HRTEM was performed with a transmission electron microscope (FEI Tecnai F30) operated at 300 kV. The Raman spectra were acquired by a JY-HR800 micro-Raman system using a laser of 633 nm. The PL emission and excitation spectra were recorded using a FLS-920T fluorescence spectrophotometer equipped with double excitation monochromators and a 450W Xe light source. The ThL experiments were performed using a ThL spectrometer (Beijing Nuclear Instrument Factory, FJ-427A) with the temperature range from 20 to 400 °C and a heating rate of 1 K/s. The rubbing activities for the ML elastomers were operated on a friction testing machine (MS-T3001; Lanzhou Huahui Instrument Technology Co., Ltd.). ML signals were *in situ* collected via an optical fiber connected with a collimator (BFC-441; Zolix Instruments Co., Ltd.). The collected signals were then transferred into a spectrometer (Omni-λ300i; Zolix Instruments Co., Ltd.) equipped with a CCD camera (iVac-316; Edmund Optics Ltd.). All digital photographs were taken by a digital camera (Canon EOS 77D).

## 2. Structural, size/morphology and elemental distribution characterizations

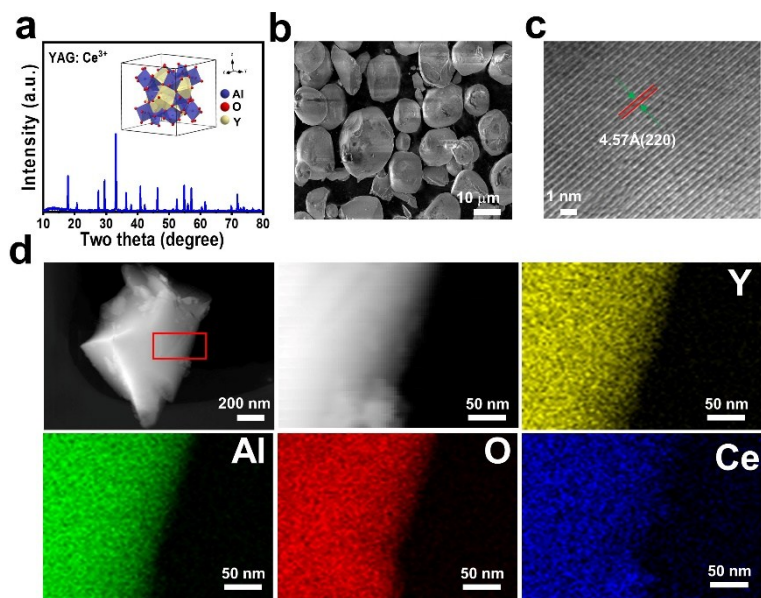


**Figure S1.** a) XRD patterns, b) SEM image (scale bar: 10  $\mu\text{m}$ ), c) HRTEM micrograph (scale bar: 1 nm), and d) elemental distribution of YAG:  $\text{Ce}^{3+}$  powders; the inset of a) presents the crystal structure of YAG.

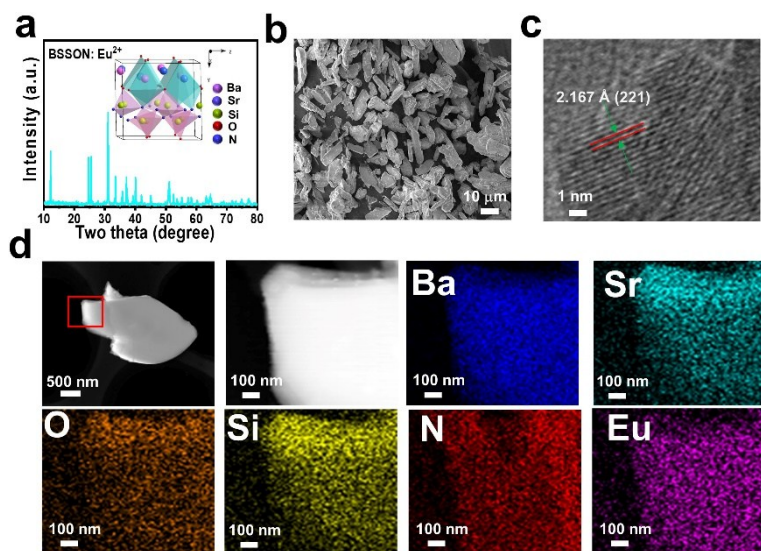


**Figure S2.** a) XRD patterns, b) SEM image (scale bar: 10  $\mu\text{m}$ ), c) HRTEM micrograph (scale bar: 1 nm), and d) elemental distribution of BSSON:  $\text{Eu}^{2+}$  powders; the inset of a) presents the crystal structure of BSSON.

### 3. ML behaviors

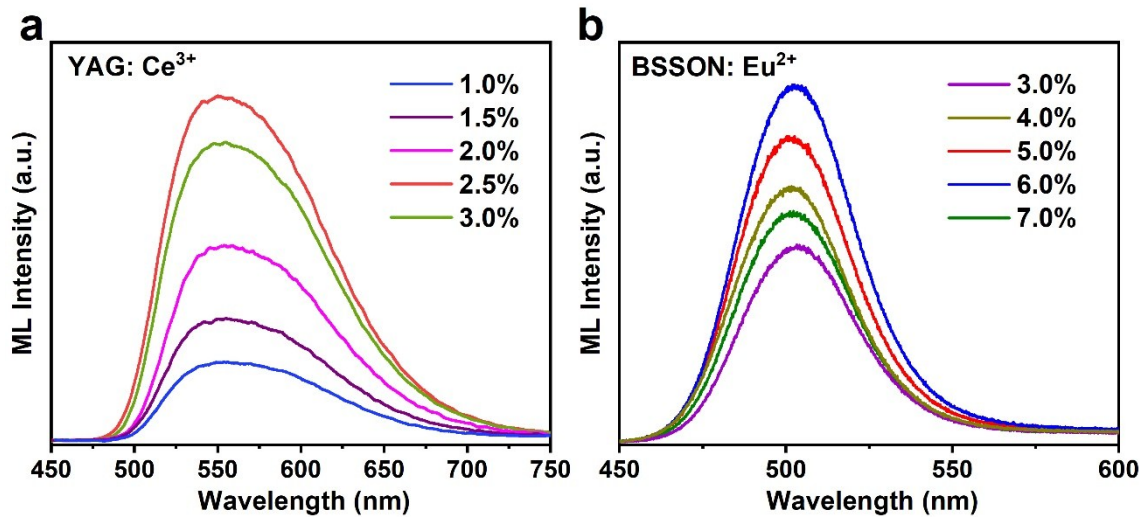


**Figure S3.** Comparison of the stretching induced ML spectra of a) YAG:  $x\text{Ce}^{3+}$  ( $x=0.01$ , 0.015, 0.02, 0.025, 0.03) and b) BSSON:  $y\text{Eu}^{2+}$  ( $y=0.03$ , 0.04, 0.05, 0.06, 0.07) under the same measurement conditions.

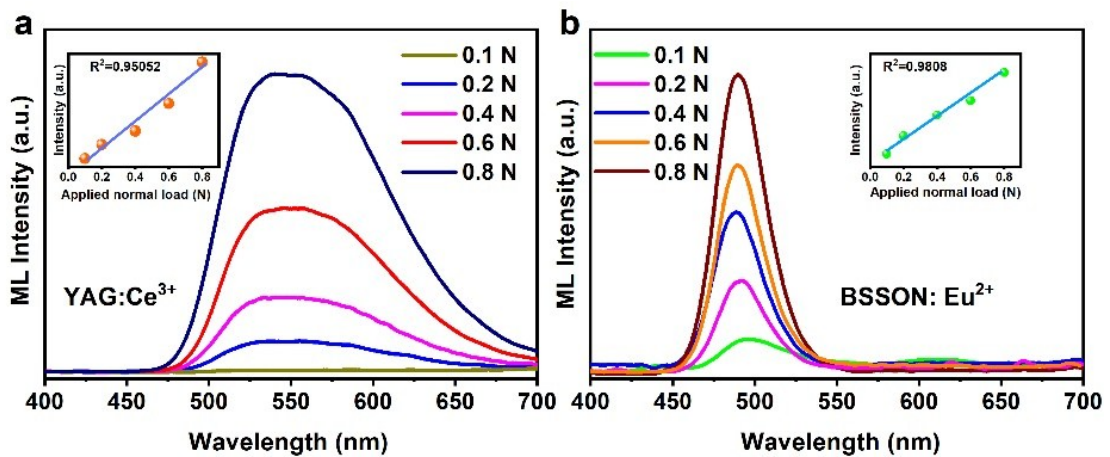


**Figure S4.** The rubbing induced ML spectra of a) YAG:  $\text{Ce}^{3+}$  and b) BSSON:  $\text{Eu}^{2+}$  under various applied normal load; the insets show the relationship between ML intensity and applied load.

#### 4. PL performance

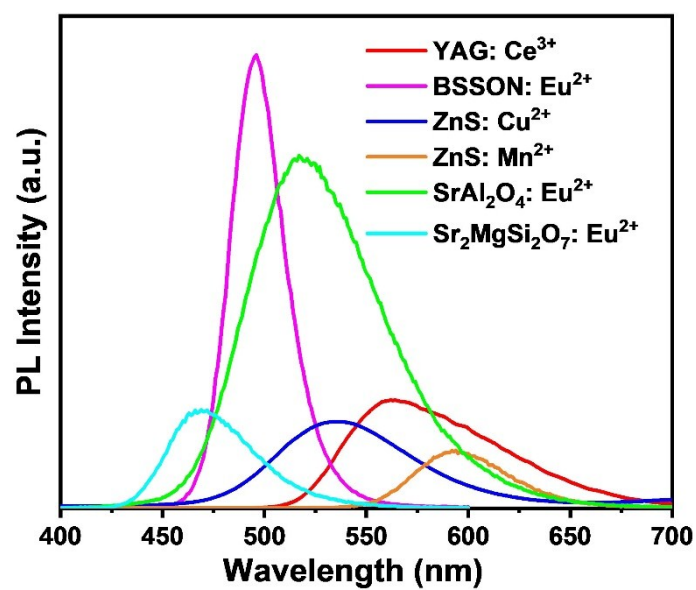


**Figure S5.** Comparison of the PL spectra of BSSON: Eu<sup>2+</sup>, YAG: Ce<sup>3+</sup>, ZnS: Cu<sup>2+</sup>, ZnS: Mn<sup>2+</sup>, SrAl<sub>2</sub>O<sub>4</sub>: Eu<sup>2+</sup> and Sr<sub>2</sub>MgSi<sub>2</sub>O<sub>7</sub>: Eu<sup>2+</sup>.

## 5. Trap analysis in structure

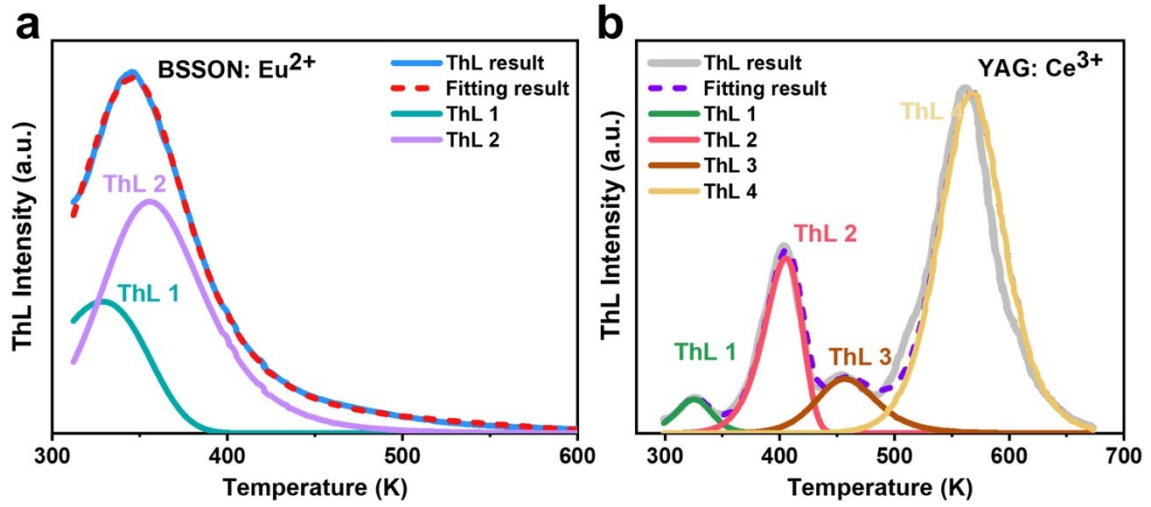


**Figure S6.** ThL curves and their fitting results of (a) BSSON:  $\text{Eu}^{2+}$  and (b) YAG:  $\text{Ce}^{3+}$  measured after a 365 nm irradiation for 10 min at room temperature.

The trap information in the structure of BSSON:  $\text{Eu}^{2+}$  and YAG:  $\text{Ce}^{3+}$ , including the trap depth and carrier density, could be revealed by analyzing the ThL curves via a classical multi-peak fitting method (Eq. S1).<sup>[1]</sup>

$$I(T) = sn_0 \exp\left(-\frac{E}{kT}\right) \left[1 + (b-1) \frac{s}{v} \times \int_{T_0}^T \exp\left(-\frac{E}{kT'}\right) dT'\right]^{-\frac{b}{b-1}} \quad (1)$$

where  $s$  is the frequency factor,  $I$  is the glow-peak intensity,  $E$  is the trap depth,  $k$  is the Boltzmann constant,  $n_0$  is the concentration of trapped carriers,  $b$  is the kinetics order parameter, and  $v$  is the heating rate ( $1 \text{ K s}^{-1}$  for our experiment). According to the work by Kitis et al.,<sup>[2]</sup> Eq. S1 could be simplified to Eq. S2. By introducing the parameters  $I_m$  and  $T_m$ , the values of  $s$  and  $n_0$  can be calculated (Eq. S3-S5), where  $T_m$  represents the temperature at the maximum and  $I_m$  is the maximum intensity of glow-peak.



$$I(T) = I_m b^{\frac{b}{b-1}} \exp\left(\frac{E T - T_m}{kT T_m}\right) \times \left[ (b-1)(1-\Delta) \frac{T^2}{T_m^2} \exp\left(\frac{E T - T_m}{kT T_m}\right) + Z \right]^{-\frac{b}{b-1}} \quad (2)$$

$$s = \frac{vE}{kT_m^2 Z} \exp\left(\frac{E}{kT_m}\right) \quad (3)$$

$$n_0 = \frac{kT_m^2}{vE} I_m Z \left(\frac{b}{Z}\right)^{\frac{b}{b-1}} \quad (4)$$

$$\Delta = \frac{2kT}{E}, \quad Z = 1 + (b-1) \frac{2kT_m}{E} \quad (5)$$

The calculated values of trap depth ( $E$ ), kinetics order parameter ( $b$ ), frequency factor ( $s$ ) and carrier density ( $n_0$ ) are summarized in Table S1. It is concluded that there are two types of traps with depths of 0.57 and 0.68 eV in BSSON: Eu<sup>2+</sup>, corresponding to the shallow and deep trap, respectively. For YAG: Ce<sup>3+</sup>, four types of traps were obtained with the trap depths of 0.65, 0.80, 0.95 and 1.30eV, respectively.

**Table S1.** Fitting parameters of ThL peaks for YAG: Ce<sup>3+</sup> and BSSON: Eu<sup>2+</sup>.

Samples	Fitting	$E$ (eV)	$b$	$s$ (s <sup>-1</sup> )	$n_0$ (cm <sup>-3</sup> )
YAG: Ce <sup>3+</sup>	ThL 1	0.65	1.53	7.09×10 <sup>9</sup>	1.01×10 <sup>6</sup>
	ThL 2	0.80	1.04	4.74×10 <sup>9</sup>	5.42×10 <sup>6</sup>
	ThL 3	0.95	1.99	2.05×10 <sup>9</sup>	2.81×10 <sup>6</sup>
	ThL 4	1.30	1.76	1.97×10 <sup>10</sup>	1.75×10 <sup>7</sup>
BSSON: Eu <sup>2+</sup>	ThL 1	0.57	1.03	2.41×10 <sup>7</sup>	1.82×10 <sup>6</sup>
	ThL 2	0.68	2.00	2.11×10 <sup>8</sup>	1.86×10 <sup>6</sup>



## 6. Raman spectra analysis

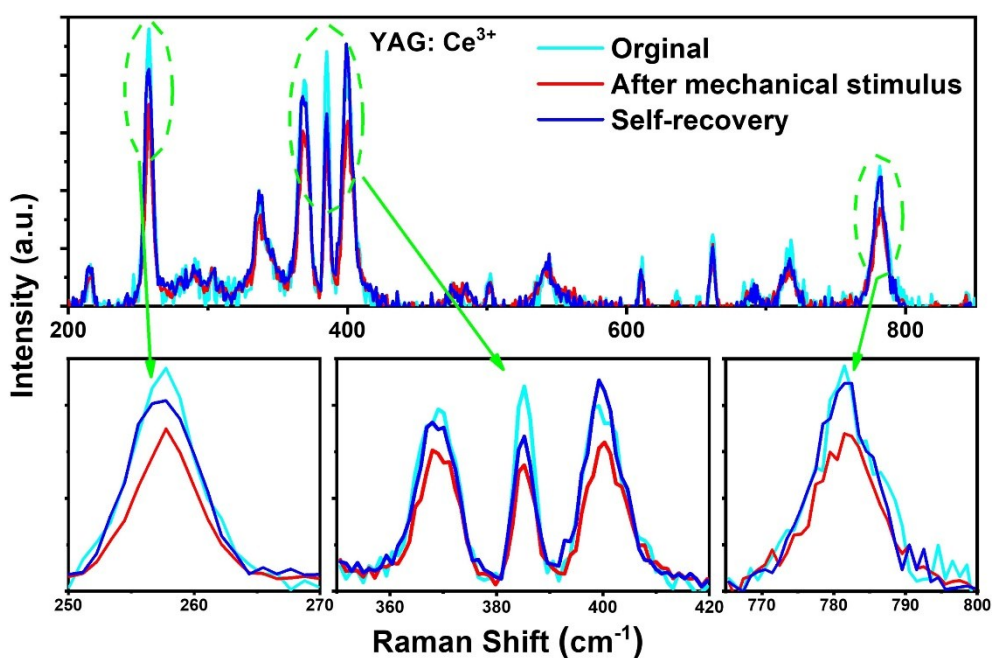


**Figure S7.** Raman spectra of YAG: Ce<sup>3+</sup> under different conditions excited by using a 633 nm laser.

After mechanical stimulus, the Raman peaks of YAG: Ce<sup>3+</sup> at 258, 369, 385, 399 and 781 cm<sup>-1</sup> decreased, suggesting the reduction of the corresponding phonon density in structure.<sup>[3]</sup> However, after the sample was placed in dark under ambient environment, all of the above Raman peaks could be almost restored to the initial ones, suggesting the phonon density recovery in the structure of YAG: Ce<sup>3+</sup>. By combining the above phenomenon with the ML properties of YAG: Ce<sup>3+</sup> in Figure 2, it is concluded that appropriate phonons in the structure of YAG: Ce<sup>3+</sup> should participate in the ML processes, which can well explain the ML decreases under continuous mechanical stimulations and its self-recovery after placing in dark under ambient environment.

## 7. Contact tracking photos based on mechanoluminescence

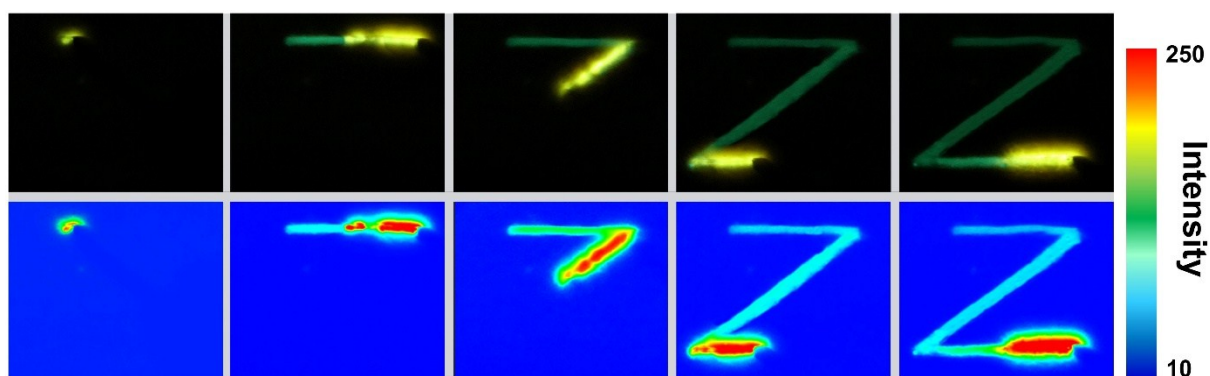


**Figure S8.** Contact tracking photographs and the corresponding luminescent mappings of the device. Green light: motion trail, greenish yellow light: contact position.

## References

- [1] R. Chen, *Journal of The Electrochemical Society* **1969**, *116*, 1254.
- [2] G. Kitis, J. M. Gomez-Ros, J. W. N. Tuyn, *Journal of Physics D: Applied Physics* **1998**, *31*, 2636.
- [3] M. J. Walter, J. M. Lupton, K. Becker, J. Feldmann, G. Gaefke, S. Höger, *Physical Review Letters* **2007**, *98*, 137401.